Emission quenching of photoactive molecules embedded in supramolecular solids: Synthesis, structure and photoluminescence studies of benzil in a CMCR-based inclusion complex with a saturated linker molecule†

Paper

Shao-Liang Zheng* and Philip Coppens*

Department of Chemistry, State University of New York at Buffalo, Buffalo, New York, 14260-3000, USA. E-mail: coppens@buffalo.edu

Using a fully saturated linker, DPP [DPP = 1,3-di-(4-piperidyl)propane], a new CMCR-based (CMCR = C-methylcalix[4]resorcinarene) supramolecular complex incorporating benzil, CMCR-DPP-benzil-EtOH-H_2O, and a corresponding benzil-free analogue CMCR-DPP-3EtOH, have been synthesized. Comparison of the TDDFT energy levels and the experimental host-absorption and guest-emission spectra, confirms that the emission quenching of benzil in a series of CMCR-linker frameworks can be attributed to the energy transfer from the guest to the host framework in the supramolecular solid and suggests strategies for increasing the lifetime of luminescent materials.

Introduction

With the rapid development of crystal engineering, photoactive species can be diluted in fully ordered host frameworks, and the guest environment can be designed such that the effect of the surrounding matrix on the photochemical properties can be examined in a systematic manner.[1] This opens the possibility for the design of solids in which host–guest energy transfer is minimized and light-emission optimized, which is relevant in the design of light-emitting diodes[2] and other optical devices.

Furthermore, we intend to apply time-resolved diffraction techniques[3] to photoactive molecules embedded in supramolecular frameworks to study the dependence of excited state geometry on the molecular environment. Information on emission quenching or enhancement is a necessary prerequisite for such studies.

It is well known that energy transfer from an excited species to the molecular environment shortens emission lifetimes and often leads to full quenching of the emission by non-radiative decay of the excited species.[4,5] The Förster mechanism[6] for energy transfer plays a major role in the quenching of fluorescence of proteins and excited species in solutions,[7] and is Coulombic in origin. However, for deactivation of triplet states Coulombic interactions that require triplet–triplet energy transitions (*i.e.* $^3D^* + {}^1A \rightarrow {}^1D + {}^3A^*$) are forbidden, and thus do not play a role. Short range energy transfer can occur through the Dexter exchange mechanism,[8] and also be mediated *via* charge-transfer (CT) configurations.[9] In both cases triplet energy transfer is allowed. Both short-range mechanisms depend on the overlap of donor and acceptor orbitals (in the supramolecular case the orbitals of the host molecules lining the guest cavity with the orbitals of the guest itself). In addition, both long and short range energy transfer depend on the energy level spacings of the donor, which is deactivated, and the acceptor.[10]

The physical properties and excited state conformation of benzil have attracted extensive attention.[11–13] Its excited triplet state has a 1.5 ms lifetime at 77 K in the solid state,[11] and a 4 ms lifetime at 17 K.[14] However, in a series of supramolecular solids based on CMCR (CMCR = C-methylcalix[4]resorcinarene) and bipyridyl-type conjugated linker molecules, the intense phosphorescence of benzil was found to be completely quenched, even at 17 K.[12] The quenching is reduced when the non-conjugated linker molecule BIMB [BIMB = 1,4-bis(imidazol-1-yl-methyl)benzene], is used to connect the CMCR molecules,[13] although even in that case the 77 K lifetime of 580 ns is very much shorter than the corresponding 1.5 ms lifetime reported for benzil at this temperature. To further investigate the effect of energy level spacings on energy transfer in solids we have synthesized a CMCR-based supramolecular solid with the fully saturated linker molecule DPP [DPP = 1,3-di-(4-piperidyl)propane] (Scheme 1), the use of which has been reported in the literature.[15] Both the benzil-free complex CMCR-DPP-3EtOH (**1**) and the corresponding host–guest system CMCR-DPP-benzil-EtOH-H_2O (**2**) and their spectroscopic properties are described below.

Experimental

Syntheses

The solid **2** was prepared by hydrothermal synthesis, previously used successfully to prepare novel resorcinarene-based supramolecular frameworks incorporating benzil.[12,13] In order to verify the spectroscopic properties of an assembly of framework-only components, complex **1** was prepared under the same conditions.
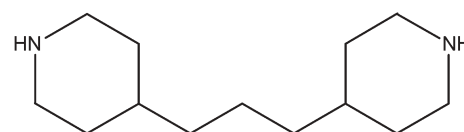
1,3-di-(4-piperidyl)propane

Scheme 1

---

† Electronic supplementary information (ESI) available: Hydrogen bonds parameters in **1** and **2** (Table S1), 2-D wave CMCR-DPP hydrogen bonded layer of **2** (Fig. S1), solid UV spectra of different linkers (Fig. S2). See http://www.rsc.org/suppdata/ce/b5/b502562a/

CMCR-DPP-3EtOH (1)

CMCR (0.05 mmol, 27.2 mg), DPP (0.05 mmol, 10.5 mg), and 4 mL of 95% ethanol solvent were sealed in a 6 mL Pyrex glass tube. The tube was allowed to stay at 120 °C for 30 h, followed by cooling to room temperature over 3 d. Yellow needle-shaped crystals appeared during the cooling period.

CMCR-DPP-benzil-EtOH-H$_2$O (2)

The procedure was identical to that for **1**, except that benzil (0.05 mmol, 10.5 mg) was added to the reaction mixture. Yellow needle-shaped crystals appeared during the cooling period.

X-Ray crystallography

Diffraction intensities for **1** and **2** were collected at 90 K on a Bruker Smart 1000 CCD area-detector diffractometer (Mo Kα, λ = 0.71073 Å), The data were integrated, scaled, sorted, and averaged using the SMART software package.[16] The structures were solved with direct methods and refined with full-matrix least-squares using SHELXTL program package.[17] Anisotropic thermal parameters were applied to all non-hydrogen atoms. The hydrogen atoms bonded to the carbons were generated at idealized positions at 0.95 Å from the corresponding C atom. The hydrogen atoms of the water molecules and the piperidyl NH hydrogens were located at the positions observed in the difference maps. Crystal data, as well as details of data collection and refinement for the complexes, are summarized in Table 1. Hydrogen bond parameters are listed in Table 1S.† Drawings were produced with Weblab Viewer Pro. 4.0.[18] CCDC reference numbers 26431 and 26432. See http://www.rsc.org/suppdata/ce/b5/b502562a/ for crystallographic data in CIF or other electronic format. These crystal data can be obtained free of charge via http://www.ccdc.cam.ac.uk/conts/retrieving.html (or from the Cambridge Crystallographic Data Center, 12 Union Road, Cambridge CB2 1EZ, UK; fax: (+44) 1223-336-033; or deposit@ccdc.cam.ac.uk).

Theoretical calculations

Time-dependent density functional (TDDFT) calculations were performed at the B3LYP level with a 6-31G** basis set, employing the Gaussian03 suite of programs.[19] Starting with the X-ray geometries, the structures were optimized by energy minimization.

Table 1 Crystal data and structure refinement of **1** and **2**

Compound	1	2
Empirical formula	C$_{51}$H$_{76}$N$_2$O$_{11}$	C$_{61}$H$_{76}$N$_2$O$_{12}$
Formula weight	893.14	1029.24
Crystal system	Monoclinic	Monoclinic
Space group	$P2_1/n$ (No. 14)	$P2_1/n$ (No. 14)
a/Å	15.4119(3)	15.6070(3)
b/Å	20.5822(4)	21.9661(4)
c/Å	16.0959(3)	15.8832(3)
β/°	91.921(1)	94.787(1)
V/Å^3	5102.9(2)	5426.2(2)
Z	4	4
ρ_{calc}/g cm^{-3}	1.163	1.260
μ/mm	0.081	0.087
Reflections collected	68164	54512
Independent reflections	9979	8505
R_{int}	0.0654	0.0609
Goodness-of-fit on F^2	1.075	1.070
R_1 [$I > 2\sigma(I)$]	0.0712	0.0508
wR_2 (all data)	0.2028	0.1450

UV-Vis reflectance and photoluminescence spectroscopy

A Perkin-Elmer Lambda 35 UV-Vis spectrometer equipped with an integrating sphere for diffuse reflectance spectroscopy was used for the UV-vis absorption experiments. The spectra were collected in the 210–800 nm range at room temperature. Powdered crystals homogeneously diluted with a non-absorbing matrix (MgO) and gently tapped into a sample holder were used as samples.

Photoluminescence measurements were carried out on a home-assembled emission detection system. Samples (several small single crystals) were mounted on a copper pin attached to a DISPLEX cryorefrigerator. A metallic vacuum chamber with quartz windows is attached to the cryostat, the chamber was evacuated to *ca.* 10^{-7} bar with a turbo-molecular pump, which allows cooling down to *ca.* 17 K. The crystals were irradiated with 366 nm light from a pulsed N$_2$-dye laser. The emitted light was collected by an Oriel 77348 PMT device, positioned at 90° to the incident laser beam, and processed by a LeCroy Digital Oscilloscope with 1–4 GHz sampling rate.

Results and discussions

Crystal structures

As shown in Table 1, both complexes crystallize in the monoclinic space group $P2_1/n$ with similar unit cells. The CMCR molecules in **1** adopt the bowl-shaped conformation with four intramolecular hydrogen bonds along their upper rim [O···O = 2.440(3)–2.729(3) Å, Table S1].† Adjacent CMCRs are connected by intermolecular hydrogen bonds [O···O = 2.459(3) and 2.532(3) Å], resulting in a 2-D wavy hydrogen-bonded layer parallel to the (010) plane, in which the CMCR molecules are oriented in an up-and-down fashion (Fig. 1). Unlike the bipyridyl-type linker molecules,[12,13] DPP does not connect adjacent CMCR layers, but further stabilizes the layer through the hydrogen bonds between one of its nitrogen atoms and hydroxyl oxygen atoms of CMCR [N(1)–H···O = 3.202(4) Å, and O–H···N(1) = 2.675(4) Å]. These hydrogen-bonded layers contain grooves parallel to the *a*-axis and are juxtaposed along the *b*-axis with a 8.0 Å (*c*/2) translation along the *c*-axis. Grooves of adjacent layers combine into channels along the *a*-axis which account for 30.1% of the crystal volume.[20] In each unit cell three ethanol molecules are clathrated in each channel and are hydrogen-bonded to the hydroxyl oxygen atoms or the second DPP nitrogen atom [O–H···O/N(2) = 2.734(3)–3.220(7) Å] of the 2-D host network.

The structure of **2** also consists of 2-D wavy hydrogen-bonded CMCR-DPP based layers (Figs. 2 and S1),† which are very similar to those in **1**. Adjacent hydrogen-bonded layers similarly combine into channels along the *a*-axis which account for 34.0% of the crystal volume. The channels are wider than in **1**, the distance between adjacent hydrogen-bonded layers being 11.0 Å, compared with 10.3 Å in **1**. The benzil molecules are embedded in the channels as dimers (Fig. 2b), formed by π–π interactions between two phenyl rings with an interplanar distance of 3.34 Å. The benzil molecules are fully ordered, the O=C–C=O torsion angles being 114.1(3)°, which is within the range of 91.8–139.3° reported for neat benzil crystals and benzil inclusion compounds.[12,13] In each unit cell one ethanol and one water molecule are also incorporated within each channel to fill the gap left by the benzil dimers, and are hydrogen-bonded to the CMCR hydroxyl oxygen atoms or DPP nitrogen atoms of the host network. As anticipated, **1** can be considered the benzil-free analogue of **2**.

Luminescence properties

In a series of supramolecular solids based on CMCR and bipyridyl-type linker molecules, the intense phosphorescence of
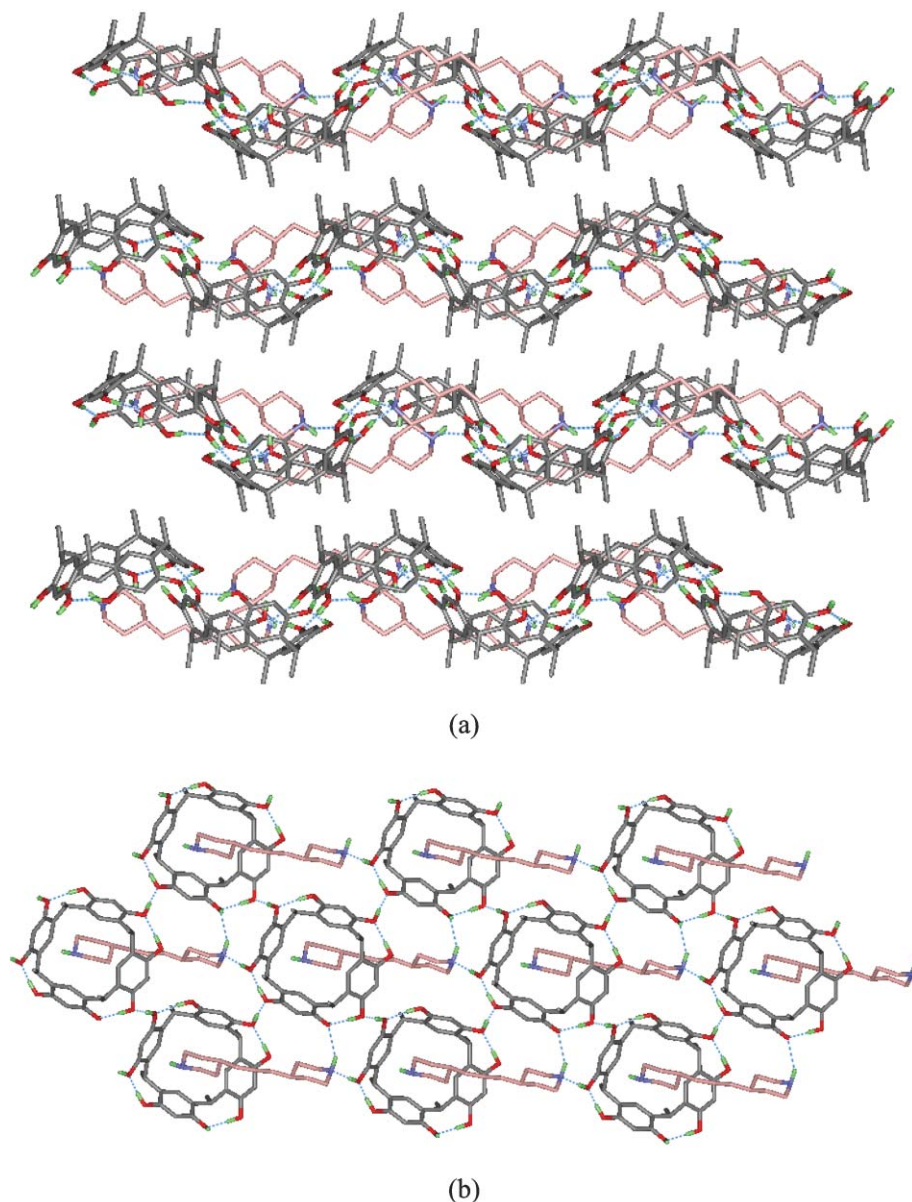
Fig. 1 (a) Three-dimensional supramolecular architecture containing channels viewed along the *a*-axis direction (*b*-axis horizontal). Click here to access a 3-D view of Fig. 1a; (b) 2-D wave CMCR-DPP hydrogen bonded layer viewed along the *c*-axis direction (*b*-axis horizontal) of **1**. Click here to access a 3-D view of Fig. 1b.

benzil was found to be completely[12] or very strongly[13] quenched, even at low temperature. Even though a non-aromatic saturated linker is used, the lifetime of benzil in **2** was found to be only 360 ns at room temperature or 580 ns at 17 K, which is similar to that of CMCR-BIMB-benzil.[13]

To explain the considerable reduction in lifetime we will examine both the experimental spectroscopic data and the theoretical energy levels of the components of the supra-molecular solid. The spectroscopic data must be used with care as the longest-wavelength absorption maxima in UV spectra will correspond to S_0–S_n transitions with $n \geqslant 1$ when the oscillator strength of the S_0–S_1 transition is small.[21] According to our TDDFT calculations, the results of which are summarized in Tables 2 and 3, this is the case for CMCR and several linker molecules. Furthermore, for triplet energy transfer the singlet–singlet energy spacings may be misleading.

The energy levels from TDDFT calculations (Tables 2 and 3) indicate that except for DPP the excited state-ground state (ES-GS) separations of isolated CMCR and linker molecules are only slightly larger than those of the benzil guest. As molecular interactions in the solid state, such as hydrogen-bonding and π–π stacking, play an important role in decreasing the ES-GS

separations such small differences for the isolated component levels are not significant.[22] Thus, if the intermolecular interactions between the CMCR and the linker molecules are taken into account, the energy gaps in the host framework may be very similar to those of the benzil guest, allowing significant energy transfer and corresponding luminescence quenching. In the current case this hypothesis can be verified spectro-scopically, as **1** can be regarded as the benzil-free analogue of **2**. Although the longest-wavelength absorption maxima in the UV spectra of **1** also correspond to S_0–S_n transitions with $n \geqslant 1$, the differences between the sum of the component spectra and that of the molecular assembly are nevertheless indicative of the effect of the interactions.

As shown in Fig. 3, neat benzil crystals emit at *ca.* 525 nm upon 337 nm excitation at room temperature,[11] and the absorption bands of a powder prepared from clear CMCR crystals[23] occur in the 210–400 nm region, whereas the absorption of the fully saturated linker, DPP ligand, lies further into the ultraviolet (210–280 nm) than the other bipyridyl-type conjugated or non-conjugated linker molecules (Fig. S2†).[12,13] However, in **1** the absorption bands have shoulders extending as far as 475 nm. Thus, the emission spectrum of the benzil
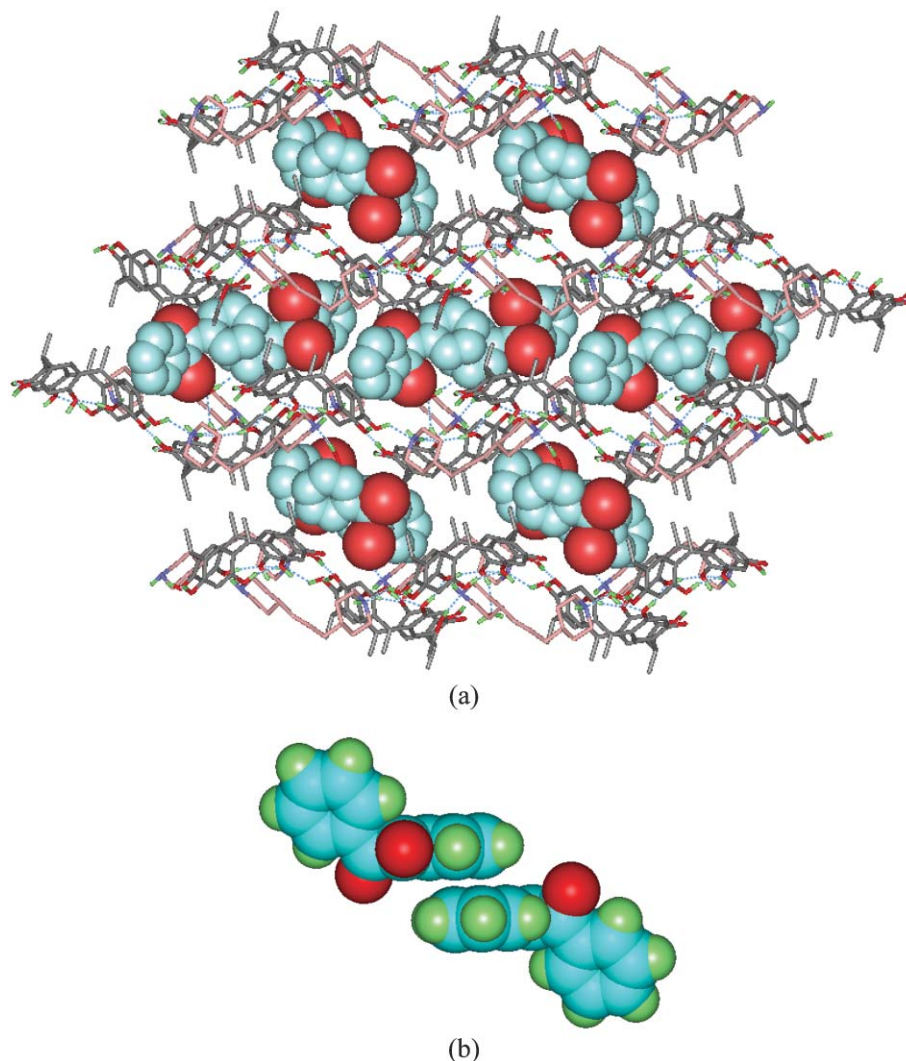
Fig. 2 (a) Three-dimensional supramolecular architecture containing channels viewed along the *a*-axis direction (*b*-axis horizontal) of **2**; (b) the dimeric benzil molecules connected by π–π interactions. Click here to access a 3-D view of Fig. 2a.

guest overlaps with the absorption spectra of the assembled framework components in **1** (Fig. 3). As the vibronic transitions of the donor (guest) and acceptor (framework) molecules overlap, significant energy transfer and corresponding luminescence quenching even involving higher energy levels with $n \geqslant 1$ is likely, in agreement with the spectroscopic observations.

Conclusions

Using a fully saturated linker, a new CMCR-based supramolecular complex **2**, and its framework-like analogue **1** have been synthesized. Though examination of the TDDFT energy levels by itself does not explain the energy transfer completely, examination of the experimental host-absorption and guest-emission spectra shows that the assembled framework components absorb further into the visible than the individual components, so that their spectrum overlaps that of benzil, in

agreement with the observed emission quenching of benzil in **2** and in other CMCR-unsaturated-linker framework solids, thus providing an explanation for the relatively low lifetime of benzil in this series of complexes.[12,13] The observed quenching contrasts the photophysical properties of ACA–benzil (ACA = apocholic acid), in which the energy level separation of the ACA host is significantly larger than that of the benzil guest molecules, and the phosphorescence lifetime of benzil at 17 K exceeds that of benzil in its neat crystal.[14] The analysis described here and those reported elsewhere[14,24] serve as a guide for strategies to be adopted in the synthesis of long-lifetime luminescent materials.

Table 2 Calculated excited state energy separations and oscillator strengths of benzil, CMCR, and DPP

Energy separation	Benzil E/eV (f)	CMCR E/eV (f)	DPP E/eV (f)
S_0–T_1	2.281 (0.000)	3.531 (0.000)	6.465 (0.000)
S_0–S_1	2.785 (0.000)	3.888 (0.000)	6.863 (0.006)
S_0–S_2	3.761 (0.001)	4.270 (0.008)	6.994 (0.018)
S_0–S_3	4.183 (0.028)	4.434 (0.036)	7.400 (0.026)

Table 3 Calculated excited state energy separations and oscillator strengths of various linker molecules

Energy separation	BPE E/eV (f)	BPEH E/eV (f)	BPY E/eV (f)	BIMB E/eV (f)
S_0–T_1	2.383 (0.000)	2.665 (0.000)	3.461 (0.000)	3.674 (0.000)
S_0–S_1	4.005 (0.001)	3.481 (0.000)	4.405 (0.005)	4.745 (0.000)
S_0–S_2	4.016 (0.003)	3.934 (0.362)	4.447 (0.002)	4.750 (0.002)
S_0–S_3	4.160 (0.899)	4.055 (0.002)	4.985 (0.005)	4.934 (0.003)
S_0–S_4	4.499 (0.045)	4.073 (0.028)	5.030 (0.037)	4.925 (0.002)
S_0–S_5	4.502 (0.000)	4.479 (0.321)	5.153 (0.000)	5.287 (0.000)
S_0–S_6	4.499 (0.000)	4.516 (0.013)	5.162 (0.000)	5.656 (0.156)

a Abbreviations: BPE = *trans*-1,4-bis(pyridyl)ethylene; BPEH = bis-(1-pyridin-4-yl-ethylidene)-hydrazine; BPY = 4,4′-bipyridine; BIMB = 1,4′-bis(imidazol-1-yl-methyl)benzene).

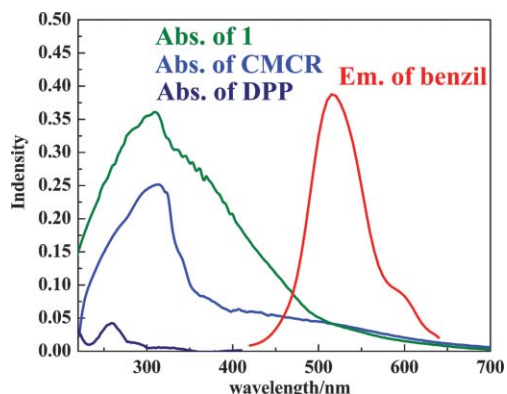**Fig. 3** The emission spectrum of the benzil guest molecules and the absorption spectra of the CMCR, DPP and **1**.

Acknowledgements

References

1 P. Coppens, B.-Q. Ma, O. Gerlits, Y. Zhang and P. Kulshrestha, *CrystEngComm*, 2002, **4**, 302–309.
2 (*a*) M. Sudhakar, P. I. Djurovich, T. E. Hogen-Esch and M. E. Thompson, *J. Am. Chem. Soc.*, 2003, **125**, 7796–7797; (*b*) I. Tanaka, Y. Tabata and S. Tokito, *Chem. Phys. Lett.*, 2004, **400**, 86–89.
3 (*a*) P. Coppens and I. V. Novozhilova, *Faraday Discuss.*, 2003, **122**, 1–11; (*b*) P. Coppens, I. I. Vorontsov, T. Graber, A. Yu. Kovalevsky, Y.-S. Chen, G. Wu, M. Gembicky and I. V. Novozhilova, *J. Am. Chem. Soc.*, 2004, **126**, 5980–5981; (*c*) P. Coppens, O. Gerlits, I. I. Vorontsov, A. Yu. Kovalevsky, Y.-S. Chen, T. Graber and I. V. Novozhilova, *Chem. Commun.*, 2004, 2144–2145; (*d*) P. Coppens, I. I. Vorontsov, T. Graber, M. Gembicky and A. Yu. Kovalevsky, *Acta Crystallogr., Sect. A*, 2005, **61**, 162–172.
4 B. Valeur, *Molecular fluorescence: principles and applications*, Wiley-VCH, Weinheim, 2002.
5 J. M. Klessinger and J. Michl, *Excited states and photochemistry of organic molecules*, VCH, New York, 1995.
6 Th. Förster, *Delocalized Excitation and Excitation Transfer, in Moldern Quantum Chemistry*, vol. 3, ed. O. Sinanoglu, Academic Press: New York, 1965, pp. 93–137.
7 R. van Grondelle and O. J. G. Somsen, *Excitation energy transfer in photosynthesis, in Resonance Energy Transfer*, ed. D. L. Andrews and A. A. Demidov, Wiley & Sons, New York, 1999.
8 D. L. Dexter, *J. Chem. Phys.*, 1953, **21**, 836–850.
9 (*a*) R. D. Harcourt, G. D. Scholes and S. Speiser, *J. Chem. Phys.*, 1996, **105**, 1897–1901; (*b*) R. D. Harcourt, G. D. Scholes and K. P. Ghiggino, *J. Chem. Phys.*, 1994, **101**, 10521–10525.
10 N. J. Turro, *Modern Molecular Photochemistry*; University Science Books: Sausalito, CA, 1991.
11 (*a*) G. Ferguson, C. Glidewell, R. M. Gregsonb and E. S. Lavenderb, *Acta Crystallogr.*, 1999, **B55**, 573–590; (*b*) P. S. Wheatley, A. J. Lough, G. Ferguson, C. J. Burchella and C. Glidewella, *Acta Crystallogr.*, 2001, **B57**, 95–102.
12 B.-Q. Ma, Y. Zhang and P. Coppens, *J. Org. Chem.*, 2003, **68**, 9467–9472.
13 B.-Q. Ma, L. F. Vieira Ferreira and P. Coppens, *Org. Lett.*, 2004, **6**, 1087–1090.
14 S.-L. Zheng and P. Coppens, unpublished results.
15 (*a*) G. Ferguson, C. Glidewell, R. M. Gregsonb and E. S. Lavenderb, *Acta Crystallogr.*, 1999, **B55**, 573–590; (*b*) P. S. Wheatley, A. J. Lough, G. Ferguson, C. J. Burchella and C. Glidewella, *Acta Crystallogr.*, 2001, **B57**, 95–102.
16 *SMART and SAINTPLUS—Area Detector Control and Integration Software*, Madison, WI, 2002.
17 G. M. Sheldrick, *SHELXTL 6.10*, Bruker Analytical Instrumentation, Madison, Wisconsin, USA, 2000.
18 *Weblab Viewer Pro. 4.0*, Molecular Simulations Inc., San Diego, CA, 1997.
19 M. J. Frisch, G. W. Trucks, H. B. Schlegel, G. E. Scuseria, M. A. Robb, J. R. Cheeseman, V. G. Zakrzewski, J. A. Montgomery, Jr., R. E. Stratmann, J. C. Burant, S. Dapprich, J. M. Millam, A. D. Daniels, K. N. Kudin, M. C. Strain, O. Farkas, J. Tomasi, V. Barone, M. Cossi, R. Cammi, B. Mennucci, C. Pomelli, C. Adamo, S. Clifford, J. Ochterski, G. A. Petersson, P. Y. Ayala, Q. Cui, K. Morokuma, D. K. Malick, A. D. Rabuck, K. Raghavachari, J. B. Foresman, J. Cioslowski, J. V. Ortiz, B. B. Stefanov, G. Liu, A. Liashenko, P. Piskorz, I. Komaromi, R. Gomperts, R. L. D. Martin, J. Fox, T. Keith, M. A. Al-Laham, C. Y. Peng, A. Nanayakkara, C. Gonzalez, M. Challacombe, P. M. W. Gill, B. Johnson, W. Chen, M. W. Wong, J. L. Andres, C. Gonzalez, M. Head-Gordon, E. S. Replogle and J. A. Pople, *GAUSSIAN03, Revision C.02*; Gaussian, Inc.: Pittsburgh, PA, 2003.
20 A. L. Spek, *PLATON, A Multipurpose Crystallographic Tool*, Untrecht University, Utrecht, The Netherlands, 2003.
21 N. J. Turro, K.-C. Liu, M.-F. Show and P. Lee, *Photochem. Photobiol.*, 1978, **27**, 523–529.
22 (*a*) P. Cassoux, *Science*, 2001, **291**, 263–264; (*b*) S.-L. Zheng, J.-P. Zhang, W.-T. Wong and X.-M. Chen, *J. Am. Chem. Soc.*, 2003, **125**, 6882–6883; (*c*) S.-L. Zheng, J.-P. Zhang, X.-M. Chen, Z.-L. Huang, Z.-Y. Lin and W.-T. Wong, *Chem. Eur. J.*, 2003, **9**, 3888–3896; (*d*) S.-L. Zheng and X.-M. Chen, *Aust. J. Chem.*, 2004, **57**, 703–712.
23 S.-L. Zheng and P. Coppens, unpublished results: CMCR-3CH$_3$CN-2H$_2$O: $a = 7.2855$ Å, $b = 19.4095$ Å, $c = 25.9748$ Å, $\beta = 97.836°$, $V = 3638.7$ Å^3.
24 S.-L. Zheng and P. Coppens, *Chem. Eur. J.*, 2005, DOI: 10.1002/chem.200500033.